Hindawi
Applied Bionics and Biomechanics
Volume 2022, Article ID 2664856, 11 pages
https://doi.org/10.1155/2022/2664856

Research Article

Biomechanical Analysis of Foot–Ankle Complex during Jogging with Rearfoot Strike versus Forefoot Strike

Yaoyong Zhang[1] and Dan Zhang[2]

[1]*College of Physical Education, Xinyang Vocational and Technical College, Xinyang 464000, China*
[2]*School of Life Sciences, Zhengzhou University, Zhengzhou 450001, China*

Correspondence should be addressed to Dan Zhang; zdxbzd@zzu.edu.cn

Received 23 August 2022; Accepted 28 October 2022; Published 19 December 2022

Academic Editor: Fuhao Mo

Background and Aim. In order to reduce foot and ankle injuries induced by jogging, two-foot strike patterns, rearfoot strike (RFS), and forefoot strike (FFS), were adopted and compared. First, RFS jogging and FFS jogging were experimentally studied, so as to acquire kinematic and kinetic data, including foot strike angle, knee flexion angle, and ground reaction force (GRF). Then, a 3D finite element model of foot–ankle complex was reconstructed from the scanned 2D-stacked images. Biomechanical characteristics, including plantar pressure, stress of metatarsals, midfoot bone, calcaneus and cartilage, and tensile force of plantar fascia and ligaments, were obtained. The results showed that RFS jogging and FFS jogging had a similar change trend and a close peak value of GRF. Since possessing more momentum in the push stage and less momentum in the brake stage, FFS jogging could be in favor of a higher jogging speed. However, FFS jogging produced larger metatarsal stress in the 5th metatarsal and much larger tensile force of plantar fascia, which might cause metatarsal fracture and heel pain. While RFS jogging produced larger plantar pressure in the hindfoot area, larger calcaneus stress, and much larger tarsal navicular stress, which might cause heel tissue injury, calcaneus damage, and stress fracture of naviculocuneiform joint. In addition, talocrural and talocalcaneal joint cartilage could bear jogging loads, as the peak contact pressure were both small in RFS jogging and FFS jogging. Therefore, jogging with rearfoot or FFS pattern should be chosen according to the health condition of foot–ankle parts.

1. Introduction

In spite of being a popular sport, running often causes injuries of foot and ankle, as which not only sustain high loads to support the body but also bear large impact from the ground [1]. Generally, foot strike pattern plays a major role in attenuating the ground impact and reducing foot and ankle injuries [2]. Thus, an increasing number of runners attempt to modify the foot strike pattern for achieving a softer landing skill [3]. As two common foot strike patterns, forefoot strike (FFS) and rearfoot strike (RFS) have different biomechanical performances, such as foot–ground interaction impact, kinetic and kinematic characteristics, internal loads in bones and tissue, Matias et al. [4].

For recommending an optimal foot strike pattern, some studies have investigated the effect of two-foot strike patterns and compared the biomechanical performance between FFS and RFS running.

As for kinematic and kinetic characteristics, different from RFS jogging, in FFS jogging, the forefoot initially contacts with the ground, it is landed with a plantarflexion posture and followed by a dorsiflexion movement [5]. Some studies have revealed that, compared with RFS running, FFS running can not only reduce the braking and impact force but also reduce the loading rate of the ground reaction force (GRF) and the knee joint force [6], as the impact is absorbed by compression of foot arch, eccentric contraction of the triceps surae, stretch of calf muscles, and Achilles tendon [7]. However, FFS running does more mechanical work (i.e., muscular work and net work of the ankle joint) and possesses higher energy expenditure, so it becomes less economical than RFS running [8, 9].

As for biomechanical characteristics, FFS running and RFS running may cause different injuries of foot bones and soft tissues, as which will bear different internal stress under two different foot strike patterns [10]. Some researchers

thought FFS running could reduce the chance of certain types of injuries and advised runners to change running style from RFS running to FFS running [11]. However, some researchers thought that compared to RFS running, FFS running would not only overload the plantar fascia and metatarsals [5, 12] but also impose threats to the foot arch and plantar connective tissues [13], so it might impose a risk of plantar fasciitis and increase the potential of metatarsal stress fracture.

Until now, most of the previous studies identified differences between FFS running and RFS running by comparing only a few parts of feet, for example, cartilage was often neglected, which might result in different or even contrary conclusions, so it is necessary to compare more parts of feet. However, even though directly responsible for injuries, the internal loads of foot and ankle, like internal stress distribution, are difficult to be in vivo measured. Because possessing the advantage of noninvasiveness, FEM overcomes the experimental limitations and provides a powerful tool for biomechanical analysis [14]. Thus, several finite element (FE) models of foot–ankle complex have been developed for predicting the internal loads in bones and tissue [15–18].

Furthermore, running has mostly been taken as the research object for comparing two-foot strike patterns. However, jogging has become increasingly popular in the past few years. As jogging often lasts longer than running, it also may produce some overuse injuries, such as plantar fasciitis, metatarsal stress fracture, and Achilles tendinitis [19]. Regrettably, only a few researchers studied jogging just for optimizing footwear [19, 20] or describing mechanics of lower extremities and lumbar spine [21, 22]. While jogging styles have not yet been compared for optimizing foot strike patterns until now.

Therefore, this study aimed to study RFS jogging and FFS jogging by experiments and simulation for reducing foot and ankle injuries. The acquired kinematic and kinetic characteristics and biomechanical characteristics could provide guidance for choosing RFS jogging or FFS jogging.

2. Methods

2.1. General Information. A male subject (age: 23 years; body mass: 76 kg; height: 1.76 m) was recruited. He was healthy without any knee and foot injuries in the past 1 year. After being fully informed of the research procedure, he signed the consent form. This study was approved by the Medicine and Life Sciences Ethics Committee of Zhengzhou University (No. 2016yxy21).

2.2. Experimental Procedure. After jogging training with RFS pattern, RFS jogging was performed at the speed of $3\,\text{m/s} \pm 5\%$ for about 3 min. Then, converted to FFS pattern and FFS jogging was performed in the same condition. The jogging speed was monitored by pairs of photoelectric cells placed along the runway and the GRF was recorded by using two adjacent force platforms (9287B, Kistler Corporation, Switzerland, 1,000 Hz). If the subject did not strike the force platform with the entire right foot or ran outside the speed range, the trial would be discarded. Whether RFS jogging or FFS jogging, the jogging trial was repeated five times. The vertical GRF threshold was set at 10 N, so the stance phase commenced when the vertical GRF exceeded 10 N and ended when it fell below 10 N. As shown in Figure 1, 39 reflective markers were placed on lower extremities and their positions were recorded by using a ten-camera motion capture system (Vicon MX, Oxford Metrics Group, UK, 200 Hz). All the raw data were processed by using Visual 3D software (C-Motion Inc., USA). With a fourth-order low-pass Butterworth filter, kinematic data and kinetic data were filtered with a cutoff frequency of 10 and 100 Hz, respectively [17, 18].

Figure 1: Reflective markers.

Two-foot strike patterns were judged by the foot strike angle (FSA), which was defined as the angle between the line connecting the two marker points at the 1st metatarsal and calcaneus and the ground surface line in the sagittal plane at initial touchdown, as shown in Figure 2. Jogging is RFS pattern when FSA is larger than 8°, while it is FFS pattern when FSA is less than –1.6°. Finally, GRF, FSA, and ankle angle were measured at two-foot strike patterns and were then used as boundary and loading conditions for further FE analysis.

2.3. FE Model

2.3.1. Model Establishment. With the subject in the supine position, the right foot–ankle was firstly fixed in a neutral posture with no load applied and then scanned by using a computed tomography (Philips Brilliance Big Bore, 120 kV, 249.48 mA, 1 mm axial slice thickness, 0.32 mm in-plane resolution). For reconstructing the geometry of a 3D foot–ankle model, firstly the scanned 2D-stacked images were imported into and processed by Mimics 17.0 (Materialise Inc., Leuven, Belgium) so as to generate 3D surfaces in STL file format, then STL files were imported into the Geomagic Studio 12.0 (Geomagic, Inc., NC, USA) for further smoothing, finally, detailed anatomic structures of 28 bones, cartilage, plantar fascia, ligaments, and soft tissue were extracted and exported in IGES file format.

Next, the IGES file was imported into ABAQUS 6.14 (Dassault Systèmes Simulia Corp., Providence, USA). Bones, cartilage, and soft tissues were meshed with linear tetrahedral elements (C3D4), as shown in Figure 3. While plantar fascia and ligaments were defined as 1D tension-only truss elements and tied to calcaneal tuberosity, proximal phalanges, soft tissues, no force emerged when they were compressed. Under a 700 N axial load, a mesh convergence test was conducted by

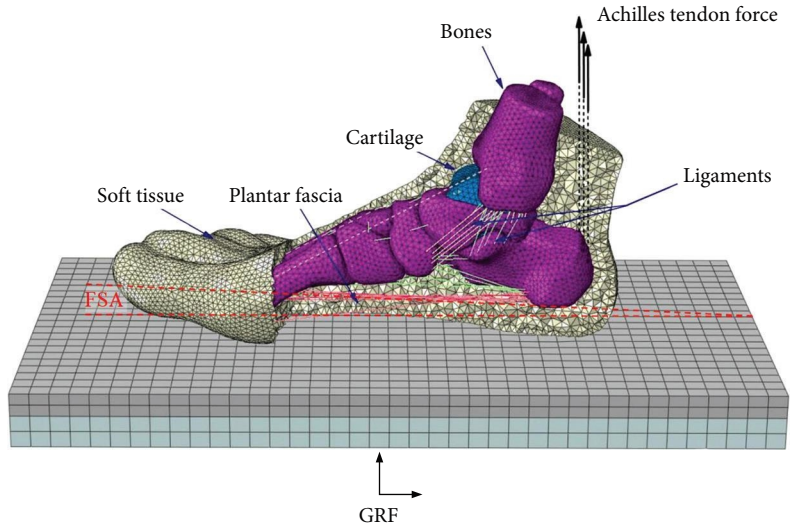

Figure 2: Finite element model of foot–ankle complex and loading conditions.

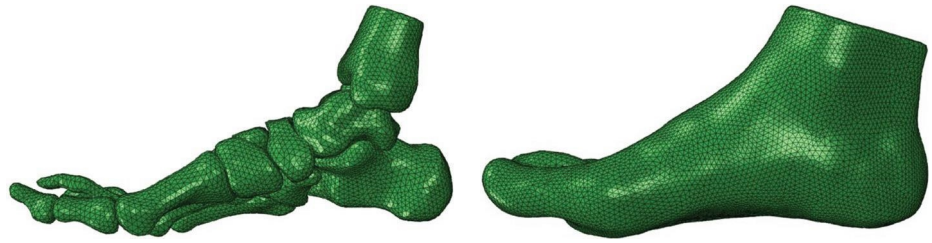

Figure 3: Mesh of (a) bones and (b) soft tissue.

Table 1: Material properties and element types [1, 15, 16].

Component	Element type	Young's modulus (MPa)	Poisson's ratio
Bones	Tetrahedron	10,000	0.34
Cartilage	Tetrahedron	45	0.4
Ligaments	Truss	260	0.4
Plantar fascia	Truss	350	0.45
Soft tissue	Tetrahedron	0.7	0.4
Ground plate	Hexahedron	17,000	0.3

gradually reducing the element size by 10% from 4 to 1 mm until the prediction outcome between two adjacent mesh sizes had less than 5% deviation. Finally, the optimal mesh size of 2 mm was chosen and a total of 273,123 elements were finally generated. All the components were defined as linear elastic isotropic materials, as shown in Table 1.

2.3.2. Boundary and Loading Conditions. Next, all the elements were imported into Abaqus 6.14 as an INP file to apply the boundary and loading conditions, as shown in Figure 2. The bone-to-bone interaction was assumed frictionless with nonlinear contact. While a hard contact between the plantar surface and the ground was defined with a friction coefficient of 0.6. The proximal cross-sectional surfaces of the tibia and fibula were constrained in 6 df. As a concentrated force, GRF was applied to the ground plate and transmitted to the plantar surface. While Achilles tendon forces were applied to the calcaneal tuberosity [23]. After the boundary and loading conditions were applied, a standard static solver was adopted and FE simulation of foot–ankle complex was performed.

2.3.3. Model Validation. For model validation, this study adopted the same boundary and loading conditions of balanced standing reported by Yu et al. [24] (i.e., constrained the proximal cross-sectional surface of the tibia and fibula in 6 df, set GRF to be 350 N and then applied it to the plantar surface). This study predicted the plantar peak pressure of 0.18 MPa, which was close to the experimental value of 0.17 MPa in the literature [24]. Furthermore, the predicted and experimental plantar pressure had a similar distribution, as shown in Figure 4. Therefore, although a little plantar pressure difference occurs because of different foot–ankles of two subjects, FE model in this study was considered valid, and the difference is considered too little to affect the findings in this study.

3. Results

3.1. Kinematic and Kinetic Analyses

3.1.1. Gait Parameters. For RFS jogging and FFS jogging, the mean FSA was $14.86 \pm 3.17°$ and $-3.71 \pm 2.05°$, respectively;

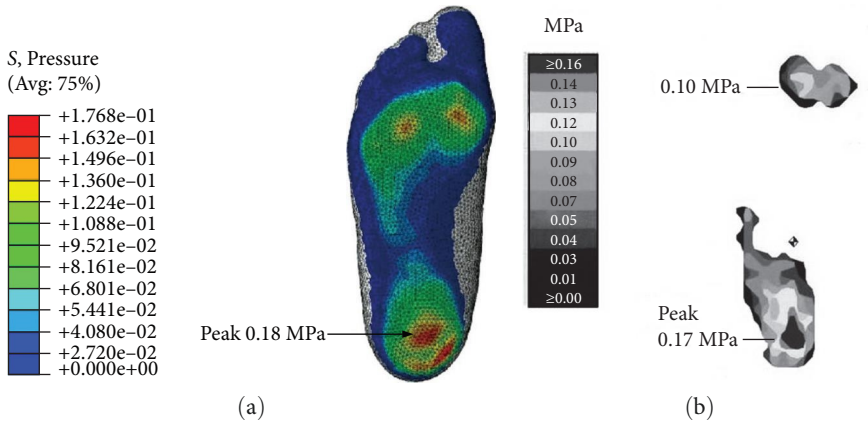

Figure 4: Comparison of (a) predicted plantar pressure in this study and (b) experimental plantar pressure tested by Yu et al. [24] under balanced standing.

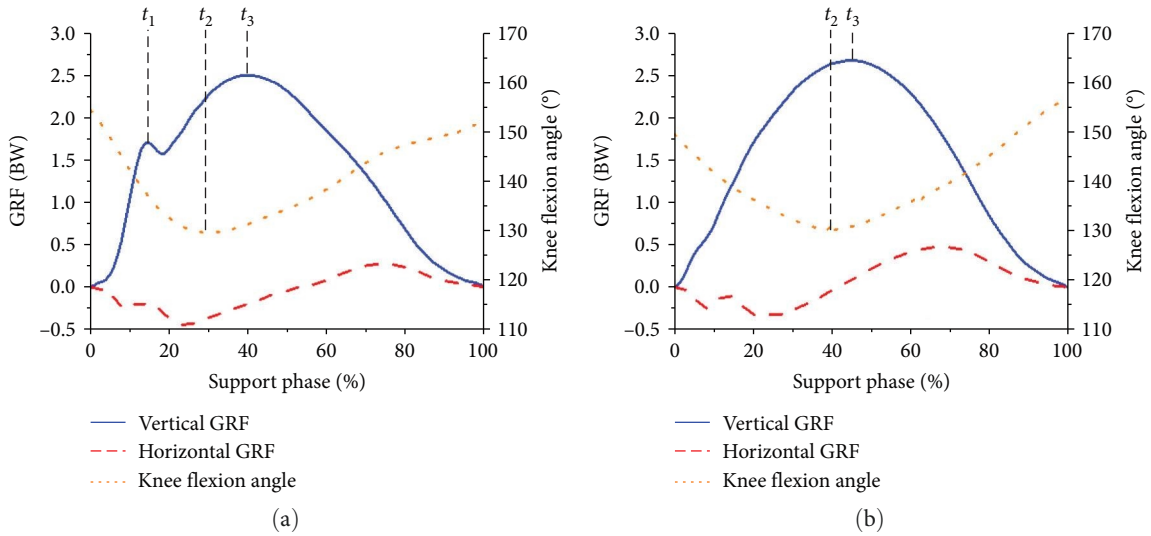

Figure 5: GRF and knee flexion angle (a) in RFS jogging and (b) in FFS jogging.

the step time was 0.67 ± 0.15 and 0.62 ± 0.03 s, respectively; the step length was 2.49 ± 0.17 and 2.34 ± 0.08 m, respectively; the mean ratio of the contact time to the flight time of one gait cycle was 0.52 and 0.54, respectively.

3.1.2. Ground Reaction Force (GRF) and Knee Flexion Angle. Because of the variable FSA during jogging, the GRF always changed. Meanwhile, the knee flexion angle also always changed. Both the GRF and the knee flexion angle would affect the biomechanical characteristics of foot–ankle complex, especially when they reached a maximum. So, GRF and knee flexion angle were analyzed next.

Whether the vertical GRF, the horizontal GRF, or the knee flexion angle, RFS jogging, and FFS jogging had a similar change trend and a close peak value, as shown in Figure 5. With the stance phase increased, the vertical GRF increased first and then decreased, it reached its maximum value at 40%–50% stance phase; while the knee flexion angle decreased first and then increased, it reached its maximum value at 30%–40% stance phase. However, some vertical GRF differences appear between RFS jogging and FFS jogging during a full gait cycle. Besides a peak vertical GRF, a relatively small peak vertical GRF, nearly 1.6 times his body weight (BW), emerged in RFS jogging because of the initial heel impact on the ground. While no other peak vertical GRF emerged in FFS jogging. Moreover, FFS jogging had a peak vertical GRF of 2.7 times BW, which was 11% larger than that in RFS jogging.

Compared to the vertical GRF, the horizontal GRF was relatively small. Whether in RFS jogging or in FFS jogging, the zero point of the horizontal GRF divided the foot strike process into two stages: brake stage (before the zero point) and push stage (after the zero point). The horizontal GRF in the brake stage and in the push stage had a similar change trend but were in opposite direction. Compared with FFS jogging, RFS jogging possessed a larger absolute peak horizontal GRF and a longer time in the brake stage, while it possessed a smaller peak horizontal GRF and a shorter time in the push stage.

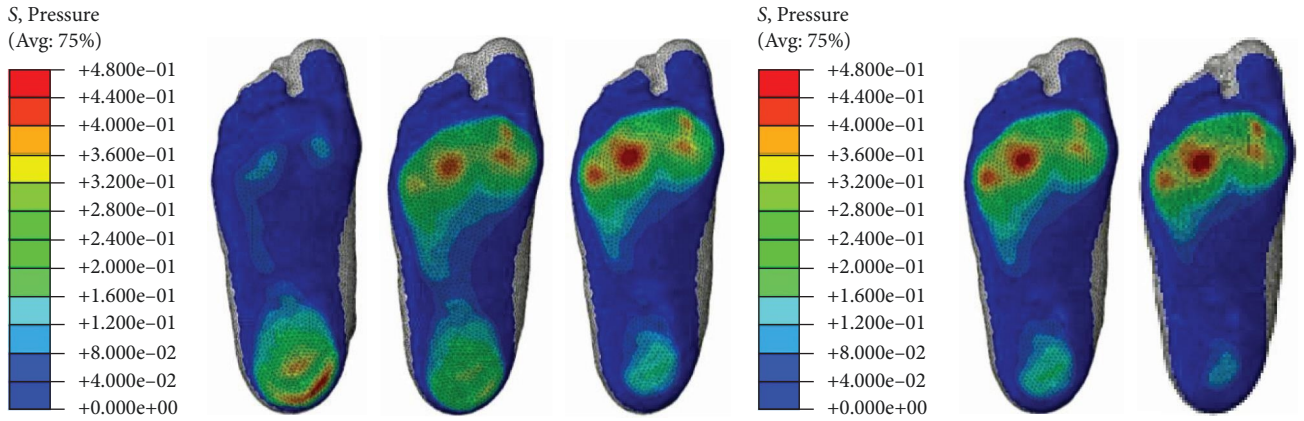

FIGURE 6: Plantar pressure distribution (a) at t_1, t_2, and t_3 gait instants in RFS jogging (from left to right) and (b) at t_2 and t_3 gait instants in FFS jogging (from left to right).

3.2. Internal Biomechanical Analysis. According to GRF and knee flexion angle, the internal biomechanics were investigated at three gait instants: t_1 for the first peak vertical GRF (only existing in RFS jogging), t_2 for the maximum knee flexion angle, and t_3 for the maximum peak vertical GRF. After performing simulation at three gait instants, internal loads, including plantar pressure, stress in bones and tissue, and tensile force of plantar fascia and ligaments, were obtained.

3.2.1. Plantar Pressure. Figure 6 shows the plantar pressure distribution in RFS jogging and FFS jogging. At t_1 gait instant, the peak plantar pressure reached 0.45 MPa and lay in the hindfoot area. At t_2 gait instant, both forefoot and hindfoot contacted with the ground in RFS jogging, so the plantar pressure lay in both forefoot area and hindfoot area; FFS jogging had a higher peak value in forefoot area and a smaller distribution area in the hindfoot area than RFS jogging. At t_3 gait instant, the plantar pressure was mainly distributed in the forefoot area and the peak plantar pressure reached its maximum value on the lateral side, whether RFS jogging or FFS jogging; moreover, the plantar pressure in RFS jogging had almost the same distribution as and a close peak value to that in FFS jogging. Because of possessing a larger vertical GRF, FFS jogging had a slightly larger plantar peak pressure of 0.47 MPa compared to RFS jogging.

3.2.2. Stress Distribution of Five Metatarsals. Figure 7 shows the stress distribution of five metatarsals in RFS jogging and FFS jogging. As the contact location changes, RFS jogging and FFS jogging had different metatarsal stress distributions at three gait instants.

In RFS jogging, the stress distribution area changed from the medial side to the lateral side. At t_1 gait instant, metatarsal stress was mainly distributed on the medial side (1st, 2nd, and 3rd metatarsals) and the 1st metatarsal had an obvious larger stress than the 2nd and 3rd metatarsals. At t_2 gait instant, the 1st and 2nd metatarsal stress decreased and the 4th and 5th metatarsal stress increased, resulting in a relatively even stress distribution among the five metatarsals. At t_3 gait instant, the 1st and 2nd metatarsal stress continued to decrease and the 4th and 5th metatarsal stress continued to increase, so that metatarsal stress was mainly distributed on the lateral side.

Because the contact location in FFS jogging always lay in the forefoot area, the metatarsal stress at t_2 gait instant had almost the same distribution as and a close peak value to that at t_3 gait instant, and the metatarsal stress was mainly distributed on the lateral side (3rd, 4th, and 5th metatarsals). The peak metatarsal stress in FFS jogging reached 34.36 MPa at t_3 gait instant and lay in the 5th metatarsal, it was much larger than that in RFS jogging.

3.2.3. Stress Distribution of Midfoot Bone. Figure 8 shows the stress distribution of midfoot bone in RFS jogging and FFS jogging. Midfoot bone consists of a tarsal navicular bone, three cuneiform bones, and a cuboid bone. Both at t_2 and t_3 gait instant, stress was mainly distributed in the tarsal navicular bone and three cuneiform bones. The peak stress at t_2 gait instant was close to that at t_3 gait instant, whether in RFS jogging or in FFS jogging. In RFS jogging, the peak stress lay in the tarsal navicular bone and reached 31.86 MPa at t_2 gait instant and 36.74 MPa at t_3 gait instant. While in FFS jogging, the peak stress also lay in the tarsal navicular bone and reached 34.62 MPa at t_2 gait instant and 34.84 MPa at t_3 gait instant. However, the peak stress did not reach its maximum value at t_2 and t_3 gait instants but at t_1 instant. At t_1 gait instant, the peak stress lay on the naviculocuneiform joint surface and reached 46.32 MPa, which is the largest stress in this study.

3.2.4. Stress Distribution of Calcaneus. Figure 9 shows the calcaneus stress distribution in RFS jogging and in FFS jogging. In RFS jogging, at t_1 gait instant, most of stress was distributed around the calcaneal tuberosity and a little was distributed around the calcaneocuboid joint, the peak calcaneus stress was 18.61 MPa; at t_2 gait instant, stress concentration emerged at the calcaneal tuberosity and the peak calcaneus stress reached its maximum value of 25.80 MPa at the attachment point of plantar fascia and ligaments; at t_3 gait instant, the peak calcaneus stress reaches 21.51 MPa at

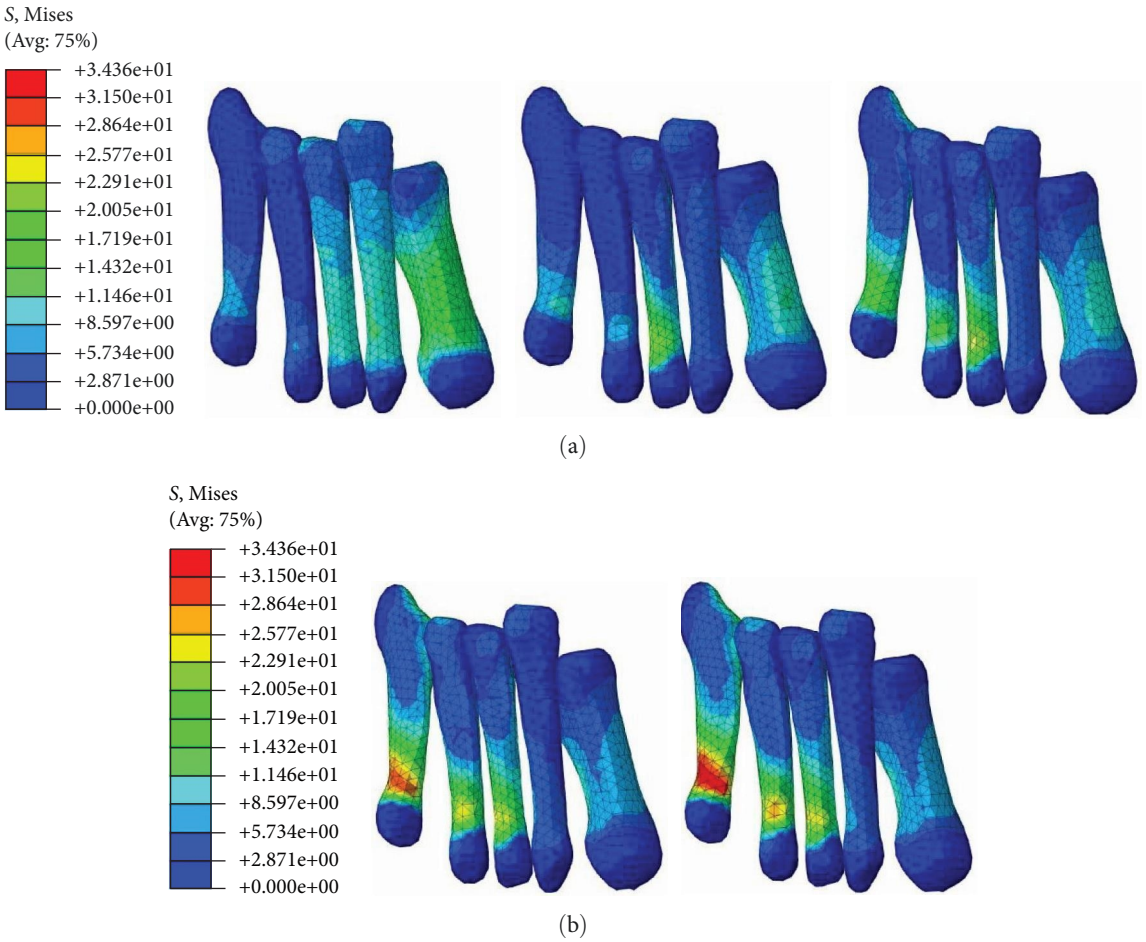

Figure 7: Stress distribution of five metatarsals (a) at t_1, t_2, and t_3 gait instants in RFS jogging (from left to right) and (b) at t_2 and t_3 gait instants in FFS jogging (from left to right).

the attachment point of Achilles tendon. In FFS jogging, the peak calcaneus stress reached 19.68 MPa at t_2 gait instant and 20.07 MPa at t_3 gait instant at the attachment point of Achilles tendon.

3.2.5. Contact Pressure Distribution of Talocrural Joint Cartilage. Figure 10 shows the contact pressure distribution of talocrural joint cartilage in RFS jogging and in FFS jogging. Compared to that at other gait instants, the contact pressure at t_1 gait instant was relatively small and its peak value was only 2.47 MPa. Whether in RFS jogging and in FFS jogging, the contact pressure at t_2 and t_3 gait instants had a similar distribution and a close peak value, and the peak contact pressure was also small. The maximum peak contact pressure was only 7.41 MPa at t_2 gait instant in FFS jogging.

3.2.6. Contact Pressure Distribution of Talocalcaneal Joint Cartilage. Figure 11 shows the peak contact pressure of talocalcaneal joint cartilage in RFS jogging and in FFS jogging. From the initial touchdown to the final liftoff, the contact pressure increased first and then decreased, whether in RFS jogging and in FFS jogging. Compared with FFS jogging, RFS jogging had a smaller peak contact pressure at the initial touchdown and at the final liftoff, while it had a larger increase rate and decrease rate. The peak contact pressure at t_2 gait instant was close to that at t_3 gait instant, whether in RFS jogging and in FFS jogging. Similarly, the peak contact pressure in RFS jogging was close to that in FFS jogging, whether at t_2 gait instant and at t_3 gait instant. Talocalcaneal joint cartilage had a larger peak contact pressure than talocrural joint cartilage, but the peak contact pressure was still small and its maximum value was only 7.21 MPa at t_3 gait instant in RFS jogging.

3.2.7. Tensile Force of Plantar Fascia and Ligaments. Table 2 shows the tensile force of plantar fascia and ligaments at t_2 and t_3 gait instants. Except plantar fascia in FFS jogging, plantar fascia and ligaments at t_3 gait instant had a larger tensile force than that at t_2 gait instant. Except long plantar ligaments, plantar fascia and ligaments in FFS jogging had a larger tensile force than those in RFS jogging. Among plantar fascia and ligaments, plantar fascia always had the largest tensile force and its tensile force reached the maximum value of 147.0 N at t_2 gait instant in FFS jogging.

4. Discussion

Because no other peak vertical GRF emerged, FFS jogging had a relatively smooth GRF curve, so it would be more stable than RFS jogging, which could attribute to the cooperative control

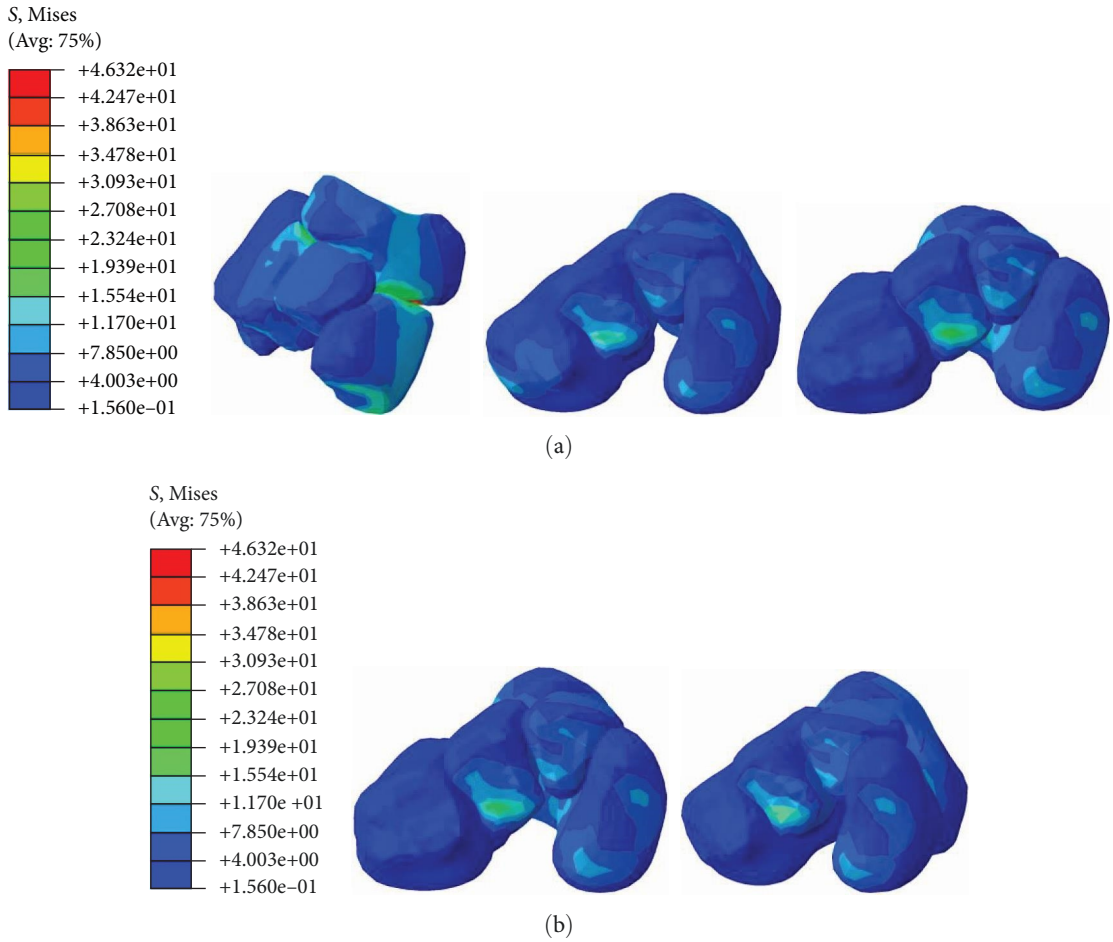

FIGURE 8: Stress distribution of mid-foot bone (a) at t_1, t_2, and t_3 gait instants in RFS jogging (from left to right) and (b) at t_2 and t_3 gait instants in FFS jogging (from left to right).

of knee extensor muscles and gastrocnemius muscle [25]. However, FFS jogging had a slightly larger peak vertical GRF, so it would be slightly higher intensive than RFS jogging.

In the brake stage, the horizontal GRF was negative, which stood for resistance. While in the push stage, the horizontal GRF was positive, which stood for assistance. By, respectively, integrating the negative value and the positive value of the horizontal GRF, the momentum in the brake stage I_a and in the push stage I_b were calculated. Because in the brake stage RFS jogging possessed a larger absolute value and a longer time than FFS jogging, so I_a in RFS jogging was larger than I_a in RFS jogging. Similarly, I_b in FFS jogging was larger than I_b in RFS jogging, Finally, I_a/I_b in RFS jogging 1.86 was much larger than I_a/I_b in FFS jogging 0.51. Because possessing more momentum in the push stage and less momentum in the brake stage, FFS jogging was in favor of a higher jogging speed.

At three gait instants, different plantar pressure distributions were presented in the hindfoot and forefoot area, which could attribute to gravity center and foot posture change in jogging. It could be concluded that the contact location in RFS jogging changed from the initial hindfoot area to both hindfoot and forefoot area to the final forefoot area; while the contact location in FFS jogging was always the forefoot area during the whole contact time [15].

The plantar peak pressure in jogging was likely two to three times that in balanced standing [26], so it would be unfavorable to our feet. For example, RFS jogging had large plantar pressure in the hindfoot area, which stood for a large impact on the hindfoot. It can be concluded that excessive RFS jogging might cause heel tissue injuries at the site of buffering effect of the plantar fat pad. While in FFS jogging almost all the plantar pressure always lay in the forefoot area during the whole contact time, which stood for a large impact on the forefoot for a long time. It can be concluded that excessive FFS jogging is unfavorable to the five metatarsals.

In FFS jogging, the peak metatarsal stress lay in the 5th metatarsal, which was corresponding to the location of the plantar peak pressure, so it could be concluded that the metatarsal stress was partially caused by the plantar pressure. Furthermore, gastrocnemius possessed high muscle activity in FFS jogging [27, 28], so a large Achilles tendon force was acquired. Then, the Achilles tendon force was enlarged by the lever action and finally transferred to five metatarsals, so it would bring an increase of the metatarsal stress. Overall, under the combined action of plantar pressure and Achilles tendon force, FFS jogging produced a much larger metatarsal stress than RFS jogging [5], so excessive FFS jogging might cause metatarsal damage, such as the 5th metatarsal fracture.

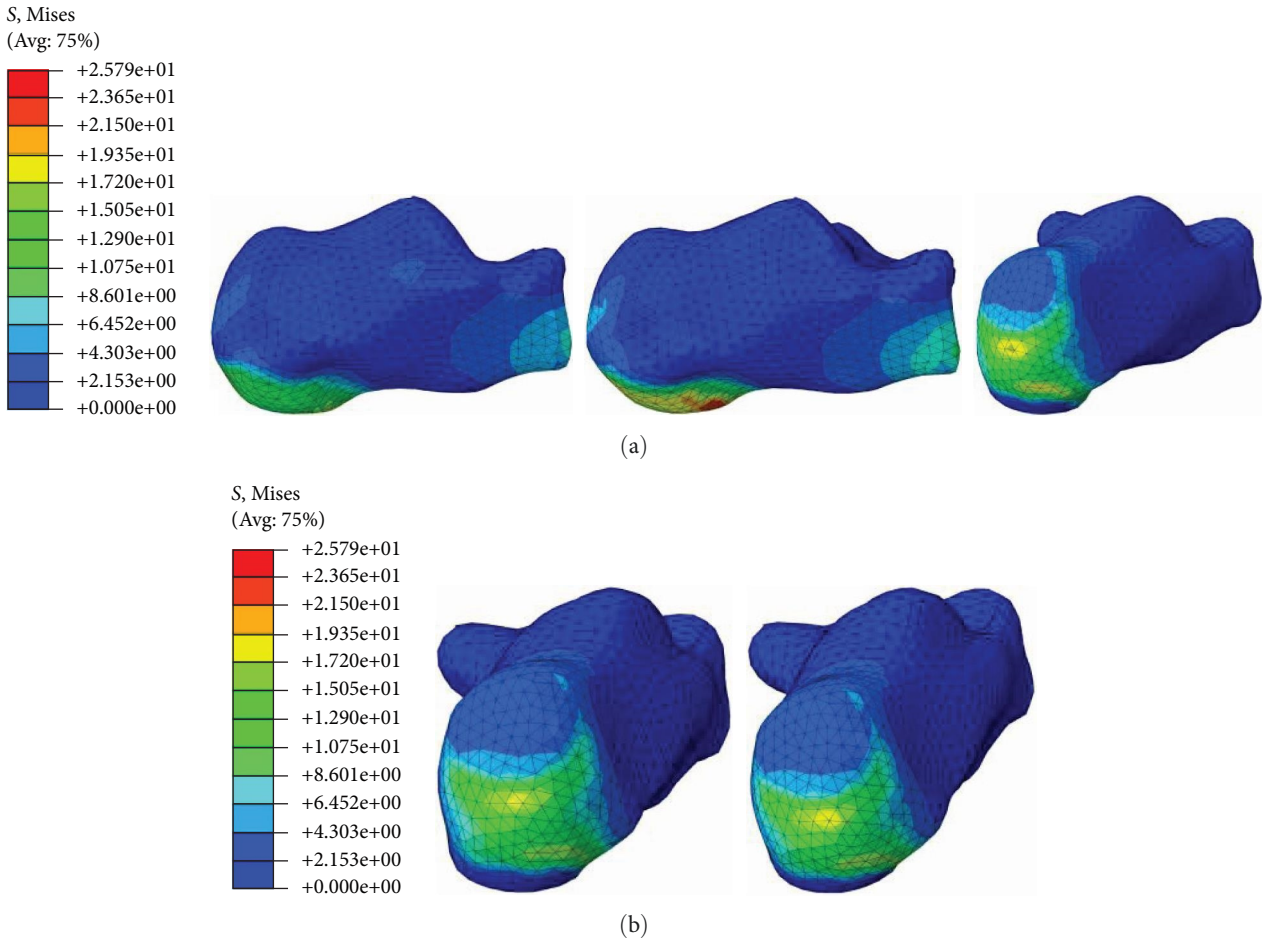

Figure 9: Calcaneus stress distribution (a) at t_1, t_2, and t_3 gait instants in RFS jogging (from left to right) and (b) at t_2 and t_3 gait instants in FFS jogging (from left to right).

While RFS jogging not only produced larger peak calcaneus stress than FFS jogging but also produced the largest stress on the naviculocuneiform joint surface, so excessive RFS jogging might cause calcaneus damage and stress fracture of the naviculocuneiform joint.

Compared to other bones, talocrural joint cartilage had a relatively even and smooth surface, so no stress concentration emerged. In addition, talus often moves around the coronal axis in the sagittal plane and rarely performs nonphysiological joint movements. Thus, the contact pressure was always small during the whole contact time, so talocrural joint cartilage could bear a large load in jogging. Moreover, the contact pressure in RFS jogging and in FFS jogging had slightly different distributions, which could attribute to the relative position change between tibia and talus under different ankle angles. Because possessing smaller contact area and bearing larger load, talocalcaneal joint cartilage had a larger peak contact pressure than talocrural joint cartilage, but the peak contact pressure was still small, so talocalcaneal joint cartilage could also bear large load in jogging.

Although possessing a close GRF, FFS jogging produced a larger tensile force of plantar fascia, plantar calcaneonavicular ligaments, and plantar cuneonavicular ligaments than RFS jogging. Especially, plantar fascia in FFS jogging had much larger tensile force than that in RFS jogging, which could also attribute to the large Achilles tendon force brought by the high muscle activity of gastrocnemius in FFS jogging. Thus, it is proved that foot posture had a greater effect on the tensile force of plantar fascia than GRF. Due to the largest tensile force of plantar fascia, FFS jogging would not be suitable for patients with plantar fasciitis [1].

Regrettably, limited by funding and time, only one subject's foot–ankle was scanned, which might lead to a little difference between simulated results and experimental results. In fact, simplified boundary conditions might have a little influence on the simulated results, for example, GRF was set as a concentrated force, which would lead to a little plantar pressure difference. However, FE model in this study was still valid, and the difference was considered too little to affect the findings in this study.

5. Conclusion

RFS jogging and FFS jogging had a similar change trend and a close peak value of GRF. Since possessing more momentum in the push stage and less momentum in the brake stage, FFS jogging would be in favor of a higher jogging speed. However, FFS jogging produced larger metatarsal stress in the 5th

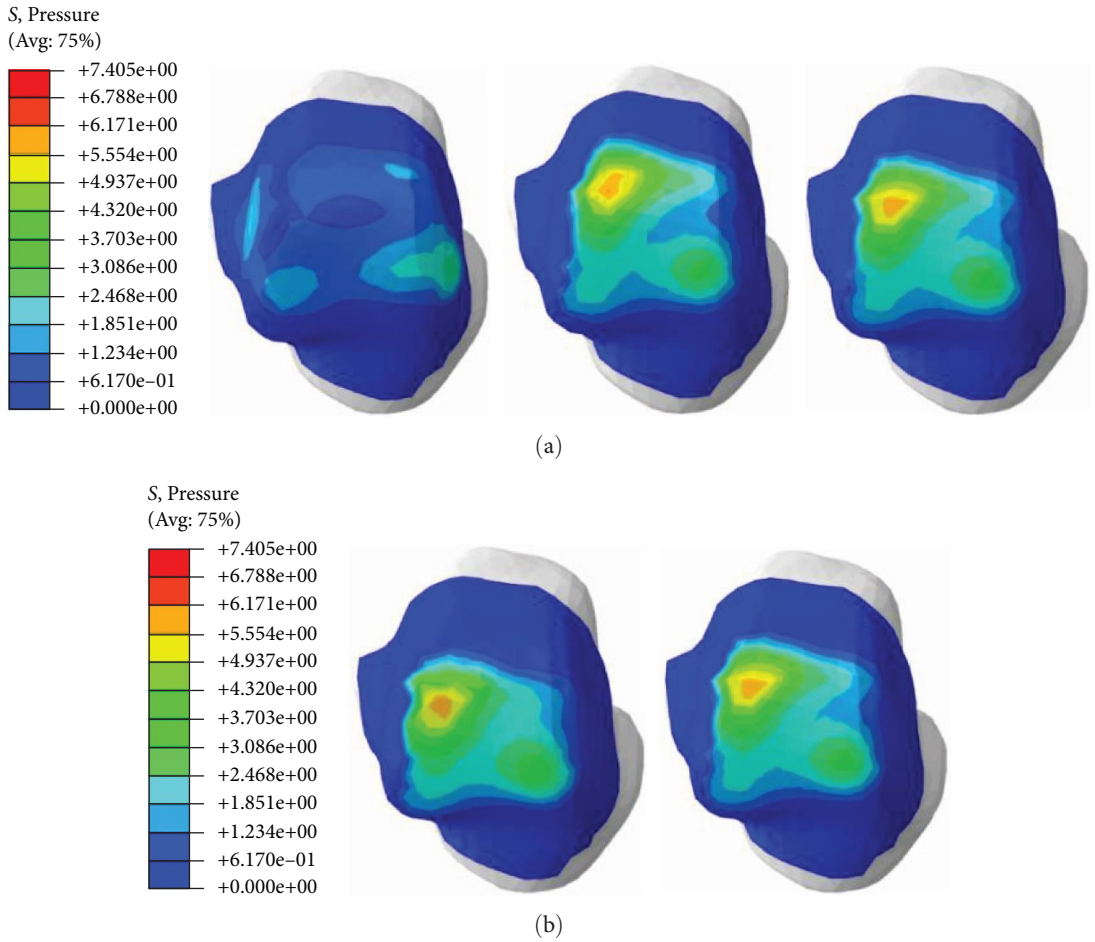

Figure 10: Contact pressure distribution of talocrural joint cartilage (a) at t_1, t_2, and t_3 gait instants in RFS jogging (from left to right) and (b) at t_2 and t_3 gait instants in FFS jogging (from left to right).

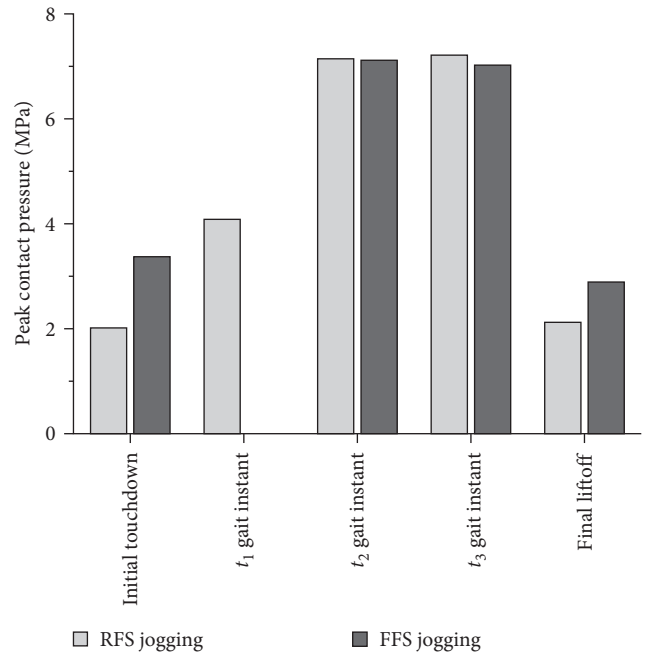

Figure 11: Peak contact pressure of talocalcaneal joint cartilage.

Table 2: Tensile force of plantar fascia and ligaments.

	RFS jogging (N)		FFS jogging (N)	
	At t_2 gait instant	At t_3 gait instant	At t_2 gait instant	At t_3 gait instant
Plantar fascia	58.3	65.1	147.0	121.2
Long plantar ligaments	16.6	35.0	16.6	19.3
Plantar calcaneonavicular ligaments	22.4	29.8	35.0	38.8
Plantar cuneonavicular ligaments	18.4	35.0	55.2	60.7

metatarsal and much larger tensile force of plantar fascia, which might cause metatarsal fracture and heel pain. While RFS jogging produced larger plantar pressure in the hindfoot area, larger calcaneus stress, and much larger tarsal navicular stress, which might cause heel tissue injuries, calcaneus damage, and stress fracture of naviculocuneiform joint. In addition, talocrural and talocalcaneal joint cartilage could bear jogging loads, as their peak contact pressure were both small in RFS jogging and FFS jogging. Therefore, jogging with rearfoot or FFS pattern should be chosen according to the health condition of foot–ankle parts.

Data Availability

The data used to support this study are available from the corresponding author upon request.

Conflicts of Interest

The authors declare that they have no conflicts of interest.

Authors' Contributions

Yaoyong Zhang and Dan Zhang contributed equally to this work.

Acknowledgments

This work was supported by the Key Scientific and Technological Project of Henan Province (No. 222102240108).

References

[1] T. L.-W. Chen, D. W.-C. Wong, Y. Wang, J. Lin, and M. Zhang, "Foot arch deformation and plantar fascia loading during running with rearfoot strike and forefoot strike: a dynamic finite element analysis," *Journal of Biomechanics*, vol. 83, pp. 260–272, 2019.

[2] Y. Uno, I. Ogasawara, S. Konda et al., "Effect of the foot-strike pattern on the sagittal plane knee kinetics and kinematics during the early phase of cutting movements," *Journal of Biomechanics*, vol. 136, Article ID 111056, 2022.

[3] K. Hébert-Losier, A. Patoz, C. Gindre, and T. Lussiana, "Foot-strike pattern at the 10 km and 39 km points of the Singapore marathon in recreational runners," *Footwear Science*, vol. 13, no. 1, pp. 43–53, 2021.

[4] A. B. Matias, P. Caravaggi, U. T. Taddei, A. Leardini, and I. C. N. Sacco, "Rearfoot, midfoot, and forefoot motion in naturally forefoot and rearfoot strike runners during treadmill running," *Applied Sciences*, vol. 10, no. 21, Article ID 7811, 2020.

[5] S. Li, Y. Zhang, Y. Gu, and J. Ren, "Stress distribution of metatarsals during forefoot strike versus rearfoot strike: a finite element study," *Computers in Biology and Medicine*, vol. 91, pp. 38–46, 2017.

[6] Y. Huang, H. Xia, G. Chen, S. Cheng, R. T. H. Cheung, and P. B. Shull, "Foot strike pattern, step rate, and trunk posture combined gait modifications to reduce impact loading during running," *Journal of Biomechanics*, vol. 86, pp. 102–109, 2019.

[7] D. E. Lieberman, M. Venkadesan, W. A. Werbel et al., "Foot strike patterns and collision forces in habitually barefoot versus shod runners," *Nature*, vol. 463, no. 7280, pp. 531–535, 2010.

[8] T. Takeshita, H. Noro, K. Hata, T. Yoshida, T. Fukunaga, and T. Yanagiya, "Muscle–tendon behavior and kinetics in gastrocnemius medialis during forefoot and rearfoot strike running," *Journal of Applied Biomechanics*, vol. 37, no. 3, pp. 240–247, 2021.

[9] J. Hamill, A. H. Gruber, and T. R. Derrick, "Lower extremity joint stiffness characteristics during running with different footfall patterns," *European Journal of Sport Science*, vol. 14, no. 2, pp. 130–136, 2014.

[10] M. J. Salzler, E. M. Bluman, S. Noonan, C. P. Chiodo, and R. J. de Asla, "Injuries observed in minimalist runners," *Foot & Ankle International*, vol. 33, no. 4, pp. 262–266, 2012.

[11] A. I. Daoud, G. J. Geissler, F. Wang, J. Saretsky, Y. A. Daoud, and D. E. Lieberman, "Foot strike and injury rates in endurance runners: a retrospective study," *Medicine & Science in Sports & Exercise*, vol. 44, no. 7, pp. 1325–1334, 2012.

[12] T. L.-W. Chen, C. E. Agresta, D. B. Lipps et al., "Ultrasound elastographic assessment of plantar fascia in runners using rearfoot strike and forefoot strike," *Journal of Biomechanics*, vol. 89, pp. 65–71, 2019.

[13] K. P. Perkins, W. J. Hanney, and C. E. Rothschild, "The risks and benefits of running barefoot or in minimalist shoes: a systematic review," *Sports Health: A Multidisciplinary Approach*, vol. 6, no. 6, pp. 475–480, 2014.

[14] Y. Li, K. Wang, L. Wang, T. Chang, S. Zhang, and W. Niu, "Biomechanical analysis of the meniscus and cartilage of the knee during a typical Tai Chi movement—brush-knee and twist-step," *Mathematical Biosciences and Engineering*, vol. 16, no. 2, pp. 898–908, 2019.

[15] F. Mo, Y. Li, J. Li, S. Zhou, and Z. Yang, "A three-dimensional finite element foot–ankle model and its personalisation methods analysis," *International Journal of Mechanical Sciences*, vol. 219, Article ID 107108, 2022.

[16] Y. Peng, D. W.-C. Wong, T. L.-W. Chen et al., "Influence of arch support heights on the internal foot mechanics of flatfoot during walking: a muscle-driven finite element analysis." *Computers in Biology and Medicine*, vol. 132, Article ID 104355, 2021.

[17] E. Morales-Orcajo, R. Becerro de Bengoa Vallejo, M. Losa Iglesias, J. Bayod, and E. Barbosa de Las Casas, "Foot internal stress distribution during impact in barefoot running as

function of the strike pattern," *Computer Methods in Biomechanics and Biomedical Engineering*, vol. 21, no. 7, pp. 471–478, 2018.

[18] C. Smolen and C. E. Quenneville, "A finite element model of the foot/ankle to evaluate injury risk in various postures," *Annals of Biomedical Engineering*, vol. 45, no. 8, pp. 1993–2008, 2017.

[19] J. Y. Qian, S. R. Shao, Y. Y. Zhang, S. Popik, and Y. D. Gu, "Biomechanics analysis of different angle of sole's toe-box region during walking and jogging," *Journal of Biomimetics, Biomaterials and Biomedical Engineering*, vol. 31, pp. 22–31, 2017.

[20] H. Branthwaite, N. Chockalingam, and A. Greenhalgh, "The effect of shoe toe box shape and volume on forefoot interdigital and plantar pressures in healthy females," *Journal of Foot and Ankle Research*, vol. 6, Article ID 28, 2013.

[21] D. Sun, F. L. Li, Y. Zhang, C. F. Li, W. L. Lian, and Y. D. Gu, "Lower extremity jogging mechanics in young female with mild *Hallux valgus*," *Journal of Biomimetics, Biomaterials and Biomedical Engineering*, vol. 22, pp. 37–47, 2015.

[22] M. E. Raabe and A. M. W. Chaudhari, "An investigation of jogging biomechanics using the full-body lumbar spine model: model development and validation," *Journal of Biomechanics*, vol. 49, no. 7, pp. 1238–1243, 2016.

[23] E. Morales-Orcajo, T. R. Souza, J. Bayod, and E. Barbosa de Las Casas, "Non-linear finite element model to assess the effect of tendon forces on the foot–ankle complex," *Medical Engineering & Physics*, vol. 49, pp. 71–78, 2017.

[24] J. Yu, J. T.-M. Cheung, Y. Fan, Y. Zhang, A. K.-L. Leung, and M. Zhang, "Development of a finite element model of female foot for high-heeled shoe design," *Clinical Biomechanics*, vol. 23, pp. S31–S38, 2008.

[25] Y. Shih, K.-L. Lin, and T.-Y. Shiang, "Is the foot striking pattern more important than barefoot or shod conditions in running?" *Gait & Posture*, vol. 38, no. 3, pp. 490–494, 2013.

[26] H. Ou, Z. Qaiser, L. Kang, and S. Johnson, "Effect of skin on finite element modeling of foot and ankle during balanced standing," *Journal of Shanghai Jiaotong University (Science)*, vol. 23, no. 1, pp. 132–137, 2018.

[27] J.-Z. Lin, W.-Y. Chiu, W.-H. Tai, Y.-X. Hong, and C.-Y. Chen, "Ankle muscle activations during different foot-strike patterns in running," *Sensors*, vol. 21, no. 10, Article ID 3422, 2021.

[28] M. Lyght, M. Nockerts, T. W. Kernozek, and R. Ragan, "Effects of foot strike and step frequency on Achilles tendon stress during running," *Journal of Applied Biomechanics*, vol. 32, no. 4, pp. 365–372, 2016.